



# Melting and undercooling of bismuth nanocrystals by solvothermal synthesis

C.D. Zou, Y.L. Gao<sup>\*</sup>, B. Yang, Q.J. Zhai

Shanghai Key Laboratory of Modern Metallurgy and Materials Processing, Shanghai University, Yanchang Road 149, Zhabei District, Shanghai 200072, PR China

## ARTICLE INFO

### Article history:

Received 8 September 2008

Received in revised form

14 July 2009

Accepted 15 July 2009

### Keywords:

Bismuth

Undercooling

Nanocrystals

Nanowires

Solvothermal synthesis

## ABSTRACT

The nanocrystals of bismuth with nanowire and sphere in shape were synthesized by solvothermal process, and it was found that the amount of nanowires would be reduced by the proper choice of the reaction solvents. The crystal structure of the as-prepared nanocrystals was investigated with X-ray diffraction (XRD). The morphology of the nanocrystals was observed with the field emission scanning electron microscope (FE-SEM). Moreover, the melting and solidification processes of the bulk bismuth and as-prepared nanocrystals were comparatively studied with differential scanning calorimetry (DSC). During the solidification process, the nanocrystals showed a larger undercooling, the value of which was about 95 and 31 °C higher than that of the bulk bismuth.

© 2009 Elsevier B.V. All rights reserved.

## 1. Introduction

Nanostructures have attracted extensive interests in recent years due to their potential use as interconnects and nanoscale electronic, optoelectronic, and sensing devices [1]. Bismuth (Bi), as a semimetal with a very small band gap, has attracted more attention recently as an interesting material for electronics due to its low effective mass, high anisotropic electronic behavior, low conduction-band effective mass, high electron mobility, and potential to induce a semimetal–semiconductor transition with decreasing crystallite size [2]. There have been some reports on the shape and size control of bismuth nanocrystals. Wang et al. [1] have reported a solution-phase process to prepare bismuth nanocrystals with the shape of wire and sphere by reducing sodium bismuthate with ethylene glycol in the presence of polyvinylpyrrolidone (PVP). Bismuth nanocubes, triangular nanoplates and nanospheres can be obtained in a polyol process by adjusting the molar ratio of PVP and bismuth [3]. By adopting high magnetic field, the shape of bismuth nanocrystals can be controlled from sphere without magnetic field to wire under high magnetic field [4]. Yet little information about their thermal stability during the heating and solidification processes was available in the aforementioned researches and thus further studies are still necessary to be conducted.

The melting properties of pure metallic small particles such as Sn [5–8], Ag [9], Cu [10], Al [11–13], In [7,14], Pb [7,15–17] Au [18,19], Bi [20–22] et al. have been studied both theoretically and

experimentally. In 1909, Pawlow derived the melting temperature of small particles as a function of surface energy and particle size, which predicted a depression of melting temperature for small particles with respect to the bulk value [23]. The size-dependent melting of bismuth nanocrystals was firstly studied with electron diffraction (ED) method on in-situ transmission electron microscope (TEM) by Takagi in 1954, which showed an experimental verification of Pawlow's prediction for the first time [24]. After Takagi, TEM has been widely used to study the size-dependent melting of small particles. Reflection high energy electron diffraction (RHEED) was also employed to probe the size-dependent melting of bismuth crystallites [25]. However, the electron beam has spurious influence on the melting behavior of small particles [16], and the diffraction technique becomes increasingly inaccurate due to line broadening as the particle size decreases [8]. Moreover, TEM cannot measure the heat associated with the melting process, because it was only limited to structural measurement. Hence, the ideal experimental technique for measuring melting of small particles is calorimetry [8]. Olson et al. [22] studied the size-dependent melting behavior of bismuth nanoparticles evaporated on a silicon nitride substrate by using nanocalorimetry. The melting behavior of bismuth nanoparticles embedded in Al and Zn matrix was studied by means of DSC [26,27]. These results clearly showed that the melting behavior depended not only on the particle size but also on the structure and excess enthalpy of the particle/matrix interface [26].

The solidification behavior of small particles has also attracted interests due to its different process in comparison with the corresponding bulk precursor. Turnbull [28] studied the formation of crystal nuclei in liquid metals and pointed out that, in large continuous masses, nucleation was almost catalyzed by

<sup>\*</sup> Corresponding author. Tel./fax: +86 21 56332144.  
E-mail address: ylgao@shu.edu.cn (Y.L. Gao).

extraneous interfaces, but for very small droplets, the probability of a catalytic inclusion presence was so little that their minimum nucleation frequencies were reproducible and therefore a consistent set of values formed. In other words, the undercooling of very small particles will be more easily obtained attributing to its homogeneous nucleation. In Takagi's study of liquid–solid transition of thin metal films by ED, the undercooling of bismuth nanocrystals was 124 °C [24]. The solidification behavior of nanoscaled bismuth particles in an Al matrix was studied by Goswami by using DSC [27], and found that the solidification of the embedded bismuth took place in a wide temperature range. The bismuth nanoparticles with a few tenths of nanometer in size embedded in germinate glass showed a large undercooling of 182 °C in value [29]. The solidification of the bismuth nanoparticles with the diameter of 22 nm embedded in Al matrix exhibited significant undercooling, with the value of 165 °C, and the degree of undercooling increased with decreasing particle size [26]. However, in the above mentioned research on Bi nanoparticles or nanocrystals, the samples were prepared directly in the measurement equipments or embedded in matrix. It is more important to consider the real word synthesis and characterization, especially the thermal stability, of the nanoparticles or nanocrystals for its application.

In this paper, the solvothermal process was employed to prepare bismuth nanocrystals, and the mixed solvents of absolute ethanol (AE) and ethylene glycol (EG) with different mixture ratios were used in different cases. The focus of the present work is, therefore, to study the melting and solidification processes of the obtained bismuth nanocrystals.

## 2. Experimental procedure

In a typical process, 0.5 g analytical grade sodium bismuthate ( $\text{NaBiO}_3 \cdot 2\text{H}_2\text{O}$ ) and 50 ml ethylene glycol (EG) were put into a beaker with the capacity of 150 ml at room temperature. The solution was then mechanically stirred intensively for 30 min. Then the resultant solution was transferred into a Teflon-lined autoclave of 45 ml capacity, and maintained at 200 °C for 24 h, followed by being naturally cooled to room temperature. In different cases, the mixed solvents of absolute ethanol (AE) and ethylene glycol (EG) with different mixing ratios, i.e. EG/AE = 3:1, EG/AE = 1:1, EG/AE = 1:3, were chosen to control the morphology of the products. After the reaction being completed, the obtained products were centrifugally separated at 4000 rpm for 20 min and rinsed for several times with large amount of absolute ethanol to remove all impurities, and then finally dried in vacuum at 60 °C for 4 h.

The products were characterized by means of X-ray diffraction from 20° to 80°, using Cu  $K_\alpha$  radiation ( $\lambda = 0.154056$  nm) on a Rigaku D/Max-2200 X-ray diffractometer. The FE-SEM (JSM-6700F) was used in order to observe the morphology of the as-prepared nanocrystals. The melting temperatures of both the nanocrystals and the bulk bismuth were measured by using a SDT-Q600 type DSC. The nanocrystals were dispersed in ethanol by means of ultrasonic vibration, and then dropped into the  $\text{Al}_2\text{O}_3$  crucible of the DSC. The sample was heated at a heating rate of 10 °C/min, from room temperature to 350 °C, and then cooled down to room temperature at the same rate, under the protection of high-purity nitrogen.

## 3. Results and discussion

On the basis of the above solvothermal process, pure bismuth nanocrystals could be obtained. Despite the mixture of nanopar-

ticles and nanowires, the crystal structures of as-prepared products could be measured by XRD. Fig. 1 shows the XRD patterns of the as-prepared products. The XRD patterns could be readily indexed to the rhombohedral phase of bismuth (JCPDS 05-0519). All the four products synthesized in different cases have the same phase, and the oxidation trace cannot be detected in the XRD patterns.

The morphology of the samples was examined by FE-SEM. Fig. 2 shows the typical SEM images of bismuth prepared in ethylene glycol and the mixed solvents of ethylene glycol and absolute ethanol at different volume ratios. The product synthesized in EG is marked as  $\text{Bi}_1$  sample. The products synthesized in the mixed solvents at different volume ratios of EG/AE = 3:1, EG/AE = 1:1, and EG/AE = 1:3 are marked as  $\text{Bi}_2$ ,  $\text{Bi}_3$ , and  $\text{Bi}_4$  samples respectively. A typical SEM image of bismuth nanocrystals synthesized in ethylene glycol ( $\text{Bi}_1$ ) is shown in Fig. 2(a), revealing the product contains a mixture of nanowires and some sub-micro and nano-sized particles. The length of the nanowires can reach several micrometers and the diameter of the nanowires is less than 100 nm. Most of the sub-micro particles are smaller than 500 nm. The typical SEM images of the products synthesized in the mixed solvents, i.e. sample  $\text{Bi}_2$ ,  $\text{Bi}_3$  and  $\text{Bi}_4$ , are shown in Fig. 2(b)–(d), respectively. By adding AE into the solvent, the morphology of the products will be controllable, which is clearly shown in Fig. 2(b)–(d). For example, with increasing of AE in the solvent, both the amount and length of the nanowires in the products are reduced. For  $\text{Bi}_3$  and  $\text{Bi}_4$  samples, the sub-micro particles are hardly to be seen, and only small amount of nanowires exist. Obviously, the products of Bi generated by solvothermal synthesis are the mixture of infinitesimal particles and nanowires, yet it offers the clear evidence to obtain fully nanoparticles of Bi by proper process control. And this, undoubtedly, supplies a promising feasible approach to prepare pure Bi nanoparticles.

In the whole synthesis process, ethylene glycol served as both solvent and reducing agent [30]. The chemical reaction can be formulated as

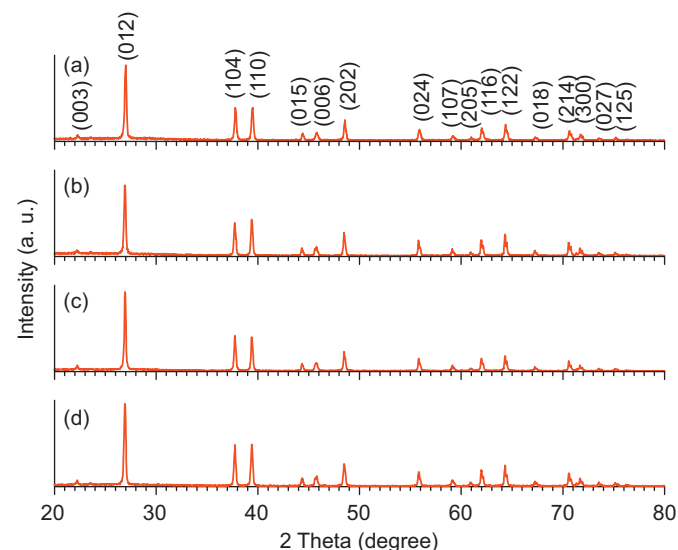
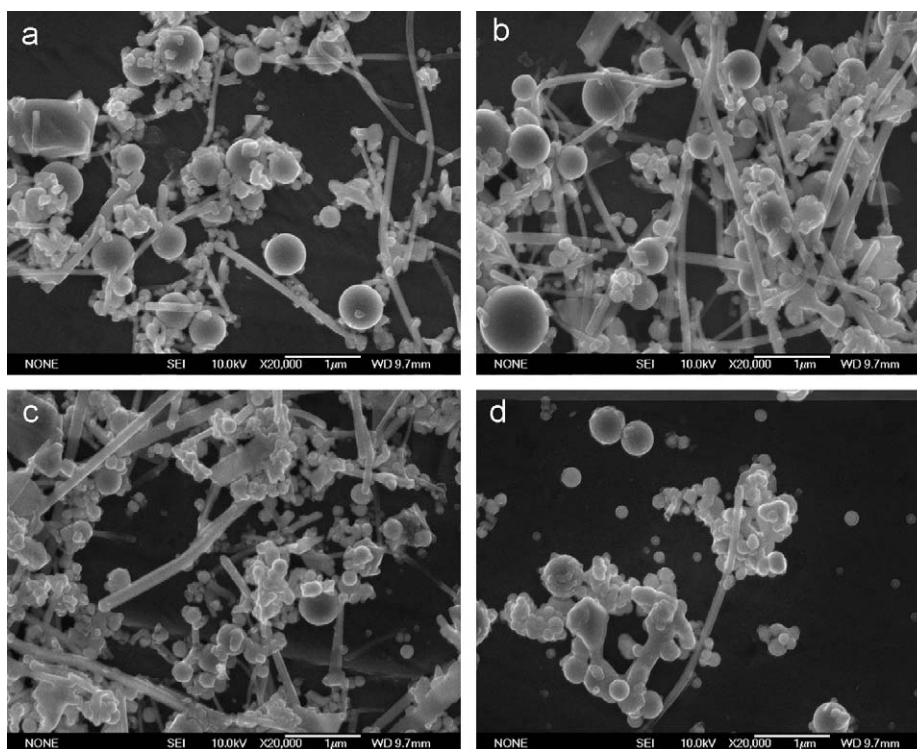


Fig. 1. XRD patterns of the products synthesized in mixed solvents of EG and AE at different volume ratios: (a) EG,  $\text{Bi}_1$ ; (b) EG/AE = 3:1,  $\text{Bi}_2$ ; (c) EG/AE = 1:1,  $\text{Bi}_3$ ; (d) EG/AE = 1:3,  $\text{Bi}_4$ .



**Fig. 2.** SEM images of Bi nanocrystals synthesized in mixed solvents of EG and AE at different volume ratios: (a) EG, Bi<sub>1</sub>; (b) EG/AE = 3:1, Bi<sub>2</sub>; (c) EG/AE = 1:1, Bi<sub>3</sub>; (d) EG/AE = 1:3, Bi<sub>4</sub>.



The formation of bismuth nanowires and nanoparticles is based on the Ostwald ripening process [31]. Bismuth nanoparticles were formed in the solution according to Eqs. (1) and (2). Some of these nanoparticles were able to grow into large crystals, serving as the seeds to continuously grow into nanowires or nanospheres.

To evaluate the particle size dependence of melting temperature or undercooling, the determination of particle size is of most important. Generally, the particle size distribution can be estimated by image analysis [32–34]. Fig. 3(a) shows the sketch of the estimation of the particle size distribution, and Fig. 3(b) shows the typical corresponding particle size histogram of Bi<sub>3</sub> sample. By using this image analysis method, the mean size of the sample can be determined as listed in Table 1.

The heating and cooling DSC curves of the bulk bismuth and as-synthesized nanocrystals are shown in Fig. 4. Fig. 4(a) and (f) show the heating and cooling DSC curves of the bulk bismuth, which indicate the onset melting temperature  $T_M$  and onset nucleation temperature  $T_N$  are 269.93 and 239.48 °C, respectively. The heating and cooling DSC curves of bismuth nanocrystals synthesized in EG are shown in Fig. 4(b) and (g), indicating that the onset melting and onset cooling temperature of these nanocrystals are 266.45 and 167.34 °C. Fig. 4(c)–(e) show the heating DSC curves of the samples synthesized in the mixed solvents of EG and AE at volume ratios: (c) EG/AE = 3:1; (d) EG/AE = 1:1; (e) EG/AE = 1:3; respectively; the corresponding cooling DSC curves are shown in Fig. 4(h)–(j), respectively. The results obtained from the DSC curves are tabulated in Table 1.

From Table 1, it can be found that the onset melting temperature of bismuth nanocrystals is about 3.5 °C lower than the bulk bismuth, showing an obvious melting temperature depression. The melting temperature depression of bismuth nanocrystals was firstly observed by ED method by Takagi [24].

The melting temperature of bismuth thin film with 5 nm mean thickness was about 23 °C lower than the bulk bismuth. The size-dependent melting temperature of bismuth nanoparticles was also studied by the newly developed means of nanocalorimetry by Allen [22], the results showed that the melting temperature of bismuth nanoparticles with 3 nm radius was about 67 °C less than the bulk bismuth. It is deemed that the relatively small melting temperature depression derives from the relative larger particle size and the coupled influence of nanowires in comparison with the results obtained by other researchers. More detailed analysis of this difference will be summarized later in this paper.

There are number of different theories on how the melting of small particles proceeds, and most of which generally predict melting temperatures in the following form [22]:

$$T_m(r) = T_m^{\text{bulk}} - \left[ \frac{2(T_m^{\text{bulk}} + 273.15)}{\Delta H_m^{\text{bulk}} \rho_s} \right] \left( \frac{\alpha}{r} \right) \quad (3)$$

where  $T_m(r)$  is the size-dependent melting temperature of the nano-particles,  $T_m^{\text{bulk}}$  is the melting temperature of the corresponding bulk precursor,  $\Delta H_m^{\text{bulk}}$  is the latent heat of melting for the bulk precursor,  $\rho_s$  is the density of the solid phase of the bulk precursor, and  $r$  is the radius. The parameter  $a$  depends on the melting model for the selected system.

For bismuth nanocrystals, the homogeneous melting model (HMM) [18] is usually applied for predicting the size-dependent melting temperature [22]. The HMM model is based on the assumption that solid and liquid particles of the same mass are in equilibrium with their common vapor, and the particles melts completely when the temperature reaches their melting temperature, without pre-melting. The parameter  $a$  in this model is determined by the following equation [18]:

$$\alpha = \sigma_{sv} - \sigma_{lv} \left( \frac{\rho_s}{\rho_l} \right)^{2/3} \quad (4)$$

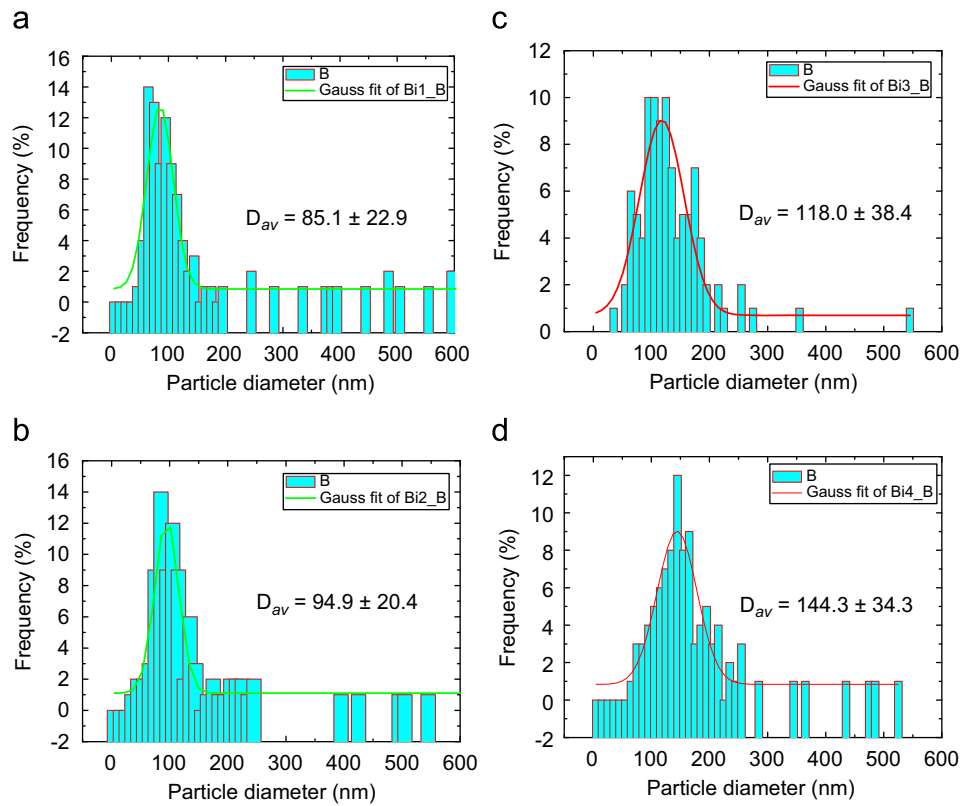


Fig. 3. The particle size histogram of samples (a) Bi<sub>1</sub>; (b) Bi<sub>2</sub>; (c) Bi<sub>3</sub>; (d) Bi<sub>4</sub>. The lines were fitted by Gaussian model.

Table 1

The results obtained from the DSC curves.

Sample	Bulk Bi	Bi <sub>1</sub>	Bi <sub>2</sub>	Bi <sub>3</sub>	Bi <sub>4</sub>
Mean particle size $D$ (nm)	$\infty$	$85.1 \pm 22.9$	$94.9 \pm 20.4$	$118.0 \pm 38.4$	$144.3 \pm 34.3$
Onset melting temperature $T_M$ (°C)	269.93	266.45	267.34	266.75	266.72
Onset nucleation temperature $T_N$ (°C)	239.48	169.74	171.93	170.73	174.78
Undercooling $\Delta T = T_M - T_N$ (°C)	30.66	96.71	95.41	96.02	91.94
Latent heat of melting $\Delta H_M$ (J/g)	40.56	25.56	26.30	23.40	29.55
Latent heat of nucleation $\Delta H_N$ (J/g)	44.17	15.46	29.95	24.99	37.38

where  $\rho_l$  is the density of the liquid phase of bulk precursor,  $\sigma_{sv}$  and  $\sigma_{lv}$  are the solid–vapor interface and liquid–vapor interface energy respectively.

Table 2 lists the data used for calculating the size-dependent melting temperatures of bismuth nanocrystals based on Eqs. (3) and (4). The melting temperature and latent heat of melting for the bulk bismuth were determined by means of DSC measurements, as given in Table 1.

Substituting the data from Table 2 into Eqs. (3) and (4), the size-dependent melting temperature of bismuth can be obtained by the following equation:

$$T_m(r) = T_m^{bulk} - \frac{248.5}{r} \quad (5)$$

Fig. 5 shows the comparison between the theoretical calculations for the size-dependent melting temperature and the experimental results determined by means of DSC for bismuth nanocrystals. It is interesting to note that the experimental values are well in agreement with the calculated ones. According to the calculated results, the melting temperature of the bismuth nanocrystals should decrease remarkably when the particle radius decreases below 75 nm. The dominating factor for the

melting temperature depression can be attributed to the increase in free energy of the nanocrystals caused by size effect.

The experimental undercooling  $\Delta T$  can be obtained according to the following equation [35]:

$$\Delta T = T_M - T_N \quad (6)$$

Here,  $T_M$  and  $T_N$  are both determined on DSC measurements.

On the basis of Eq. (6) combined with the DSC measurement, the undercooling  $\Delta T$  of the bulk bismuth and the as-synthesized nanocrystals can be obtained, as listed in Table 1. The undercooling  $\Delta T$  of the bulk bismuth was only 30.66 °C. However, the undercooling of the nanocrystals, e.g., 96.71 °C for the nanocrystals synthesized in EG, was much larger than that of the bulk bismuth. In contrast, the undercooling of bismuth thin film with mean thickness of 5 nm was 147 °C, which was ever demonstrated by Takagi [24] by means of in-situ transmission electron microscope (TEM), implying that smaller particle size is helpful to increase the undercooling.

According to Turnbull's theory, two steps of solidification of pure metals should be taken into account: nucleation of crystals and their subsequent growth [28]. The rate of solid formation is mainly determined by the rate of nucleation because the latter step occurs so rapidly. Since bulk metals are expected to contain

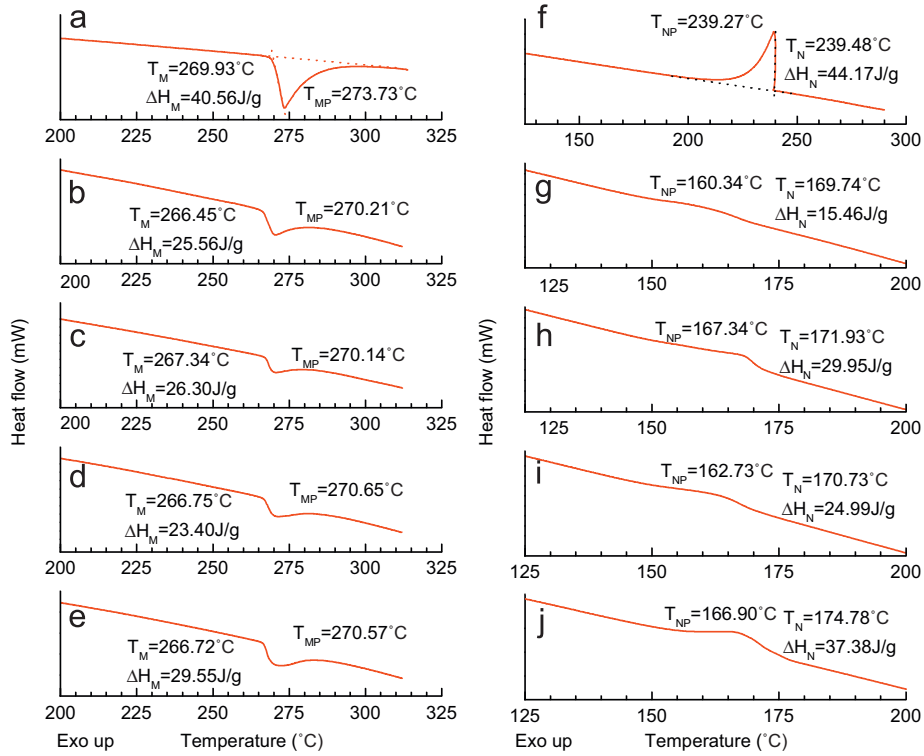


**Fig. 4.** The heating and cooling DSC curves of the bulk bismuth and as-synthesized bismuth nanocrystals (a)–(e): heating DSC curves; (a) bulk bismuth; (b) Bi<sub>1</sub>; (c) Bi<sub>2</sub>, (d) Bi<sub>3</sub> and (e) Bi<sub>4</sub>; (f)–(j) the corresponding cooling DSC curves.

**Table 2**  
Data used in calculating bismuth aimed at Eqs. (1) and (2) [37].

$T_m^{bulk}$	$\Delta H_m^{bulk}$	$\rho_s$	$\rho_l$	$\sigma_{sv}$	$\sigma_{lv}$
269.93 °C	40.56 J/g	9.7 g/cm <sup>3</sup>	10.07 g/cm <sup>3</sup>	550 mJ/m <sup>2</sup>	378 mJ/m <sup>2</sup>

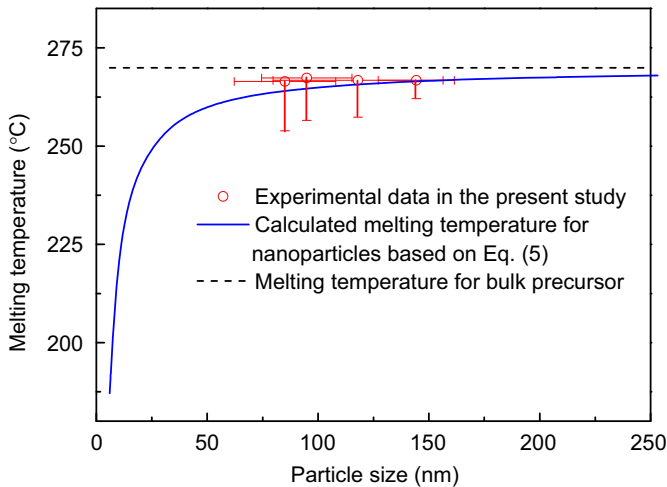


**Fig. 5.** Theoretical calculated and experimental results for the melting temperature versus the particle size.

sufficiently many accidental inclusions of external origin, effective as nuclei of crystallization, the undercooling is unusually observed [24]. For bismuth, when homogeneous nucleation occurs during the solidification process, the undercooling will be reached at 90 °C [28], with the ratio of  $\Delta T/T_M$  being 0.165. In other words, if the ratio of  $\Delta T/T_M$  is larger than 0.165, the homogeneous

nucleation will occur during the bismuth solidification process. In this work, the bismuth nanocrystals show larger undercooling during its cooling process of the DSC measurement. For Bi<sub>1</sub> sample, the undercooling is 96.71 °C with the ratio of  $\Delta T/T_M$  0.179, indicating the homogeneous nucleation occurs during its solidification process.

In general, undercooling is attributed to the presence of a nucleation barrier during solidification process that results from the competition between the decrease in the volume free energy upon solidification and the increase in the free energy associated with the existence of a solid–liquid interface [25]. Basing on the classical homogeneous nucleation theory, Sheng et al. [26] obtained the relationship between undercooling of small particles and its size, which can be written as the following equation:

$$\Delta T_{(r)} = \Delta T^{bulk} + \frac{T_m^{bulk}}{\rho \Delta H_m^{bulk}} \frac{3\alpha \Delta \sigma}{r} \quad (7)$$

where  $\Delta T_{(r)} = T_M - T_N$  is the undercooling of nanocrystals with the radius of  $r$ ,  $\Delta T^{bulk}$  is the undercooling of “bulk” precursor ( $r \rightarrow \infty$ ),  $a$  is the fraction of the liquid/matrix interface that is replaced by the solid/matrix interface after solid nucleation with the value between 0 and 1, in this work,  $a = 1$  was used because the bismuth nanocrystals were assumed to be free in the DSC pan.  $\rho$  is defined as the average density of solid and liquid phase, i.e.  $\rho = \frac{1}{2}(\rho_s + \rho_l)$ , and  $\Delta \sigma = \sigma_{sv} - \sigma_{lv}$ . Then, the undercooling of bismuth nanocrystals as a function of crystal size can be obtained easily by the equation

$$\Delta T_{(r)} = \Delta T^{bulk} + \frac{698.94}{r} \quad (8)$$

Fig. 6 shows the calculated undercooling of bismuth nanocrystals as a function of crystal size, the solid circle represents the experimental results estimated by DSC, the solid line and dotted line represent the calculated results by using

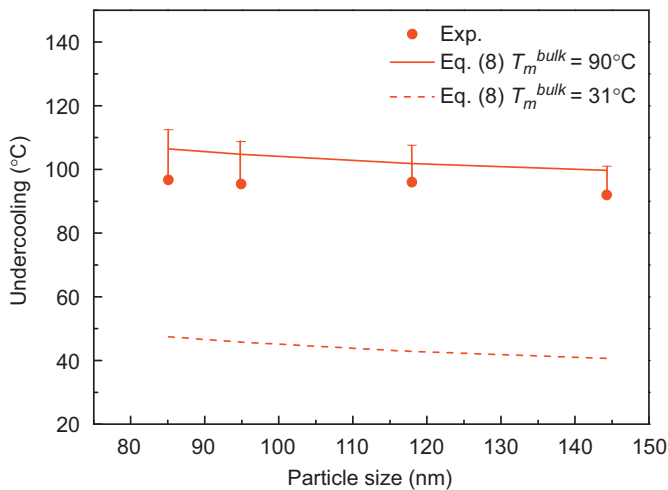


Fig. 6. Undercooling of bismuth nanocrystals as a function of crystal size estimated by Eq. (8).

$\Delta T^{bulk} = 90^\circ\text{C}$  [28], the maximum undercooling of bismuth corresponding to a temperature at which the homogenous nucleation becomes appreciable, and  $31^\circ\text{C}$ , determined by DSC in this work, respectively. From Fig. 6, it is found that the experiment results were much larger than the calculated ones when the value of  $31^\circ\text{C}$  was used for the calculation of Eq. (8). However, in this work, the real bulk bismuth was used for the comparative study of the solidification process of bulk bismuth and bismuth nanocrystals. In Lu's model, the undercooling of "bulk" materials was the undercooling of microparticles [26], which will be much larger than the real bulk materials due to the size effect on the undercooling of molten metals [36]. Hence, the value of  $\Delta T^{bulk}$  should be determined by the maximum undercooling of bulk bismuth, the value of which was  $90^\circ\text{C}$ , given by Turnbull [28]. If the maximum undercooling of bulk bismuth was used, it would be found that the experimental results were perfectly agreed with the calculated ones.

#### 4. Conclusions

The bismuth nanocrystals have been obtained by solvothermal synthesis. With increasing the ratio of AE in the applied mixed solvents, the morphology of the bismuth nanocrystals reveals the tendency to change from wire to sphere and also the size decrease of the sphere will also be obtained, indicating the promising feasibility to prepare fully nanoparticles of bismuth by this technique.

Due to the existence of nanowire and the large size of the crystals, the melting temperature depression of the bismuth nanocrystals was only about  $3.5^\circ\text{C}$ , in agreement with that calculated by homogeneous melting model.

The solidification undercooling of the bismuth nanocrystals obtained by DSC measurement showed that the value of the undercooling of bismuth nanocrystals was much higher than that of bulk bismuth at a cooling rate of  $10^\circ\text{C}/\text{min}$ . Besides, the obtained experimental size-dependent undercooling was in accordance with that of the theoretically estimated results.

#### Acknowledgments

This work was supported by the National Natural Science Foundation of China (Grant no. 50571057), AM Foundation (Grant no. 08520740500), Shanghai Rising-Star Program (Grant no. 06QA14020) and Shanghai Municipal Education Commission Program (Grant no. 2006AZ002).

#### References

- [1] J. Wang, X. Wang, Q. Peng, et al., *Inorg. Chem.* 43 (2004) 7552.
- [2] J. Fang, K.L. Stokes, J.A. Wiemann, et al., *Mater. Sci. Eng. B* 83 (2001) 254.
- [3] W.Z. Wang, B. Poudel, Y. Ma, et al., *J. Phys. Chem. B* 110 (2006) 25702.
- [4] Y. Xu, Z. Ren, W. Ren, et al., *Nanotechnology* 19 (2008) 115602.
- [5] T. Bachelis, H.-J. Gutherodt, R. Schaer, *Phys. Rev. Lett.* 85 (2000) 1250.
- [6] C.R.M. Wronski, *Br. J. Appl. Phys.* 18 (1967) 1731.
- [7] G.L. Allen, R.A. Bayles, W.W. Gile, et al., *Thin Solid Films* 144 (1986) 297.
- [8] S.L. Lai, J.Y. Guo, V. Petrova, et al., *Phys. Rev. Lett.* 77 (1996) 99.
- [9] M. Quaaas, I. Shyjumon, R. Hippler, et al., *Z. Kristallogr.* 26 (Suppl.) (2007) 267.
- [10] L. Wang, Y. Zhang, X. Bian, et al., *Phys. Lett. A* 310 (2003) 197.
- [11] J. Sun, S.L. Simon, *Thermochim. Acta* 463 (2007) 32.
- [12] S.L. Lai, J.R.A. Carlsson, L.H. Allen, *Appl. Phys. Lett.* 72 (1998) 1098.
- [13] S. Arai, S. Tsukimoto, H. Saka, *Microsc. Microanal.* 4 (1998) 264.
- [14] M. Dippel, A. Maier, V. Gimple, et al., *Phys. Rev. Lett.* 87 (2001) 095505.
- [15] F.P. Kevin, C. Yip-Wah, B.C. Jerome, *Appl. Phys. Lett.* 71 (1997) 2391.
- [16] K.F. Peters, J.B. Cohen, Y.-W. Chung, *Phys. Rev. B* 57 (1998) 13430.
- [17] K.C. Prince, U. Breuer, H.P. Bonzel, *Phys. Rev. Lett.* 60 (1988) 1146.
- [18] P. Buffat, J.P. Borel, *Phys. Rev. A* 13 (1976) 2287.
- [19] Y. Wang, S. Teitel, C. Dellago, *Chem. Phys. Lett.* 394 (2004) 257.
- [20] E. Haro-Poniatowski, M. Jouanne, J.F. Morhange, et al., *Phys. Rev. B* 60 (1999) 10080.
- [21] E. Haro-Poniatowski, R. Serna, C.N. Afonso, et al., *Thin Solid Films* 453–454 (2004) 467.
- [22] E.A. Olson, M.Y. Efremov, M. Zhang, et al., *J. Appl. Phys.* 97 (2005) 034304.
- [23] Q.S. Mei, K. Lu, *Prog. Mater. Sci.* 52 (2007) 1175.
- [24] M. Takagi, *J. Phys. Soc. Jpn.* 9 (1954) 5.
- [25] M.K. Zayed, H.E. Elsayed-Ali, *J. Appl. Phys.* 99 (2006) 123516.
- [26] H.W. Sheng, K. Lu, E. Ma, *Acta Mater.* 46 (1998) 5195.
- [27] R. Goswami, K. Chattopadhyay, *Acta Mater.* 52 (2004) 5503.
- [28] D. Turnbull, *J. Appl. Phys.* 21 (1950) 1022.
- [29] E. Haro-Poniatowski, M. Jimenez De Castro, J.M. Fernandez Navarro, et al., *Nanotechnology* 18 (2007).
- [30] P. Toneguzzo, G. Viau, O. Acher, et al., *Adv. Mater. (Weinheim, Ger.)* 10 (1998) 1032.
- [31] A.R. Roosen, W.C. Carter, *Physica A (Amsterdam)* 261 (1998) 232.
- [32] R. Fisker, J.M. Carstensen, M.F. Hansen, et al., *J. Nanopart. Res.* 2 (2000) 267.
- [33] E. Muthuswamy, S. Ramadevi, H.N. Vasan, et al., *J. Nanopart. Res.* 9 (2007) 561.
- [34] J. Muñoz, J. Cervantes, R. Esparza, et al., *J. Nanopart. Res.* 9 (2007) 945.
- [35] B.A. Mueller, J.H. Perepezko, *Metall. Trans. A* 18 (1987) 1143.
- [36] W. Guan, Y. Gao, Q. Zhai, et al., *J. Mater. Sci.* 39 (2004) 4633.
- [37] N.B. Thoft, J. Bohr, B. Buras, et al., *J. Phys. D: Appl. Phys.* 28 (1995) 539.